Laser and Particle Beams (2006), *24*, 503–509. Printed in the USA.

DOI: 10.1017/S0263034606060666

A pulsed power generator for x-pinch experiments

XIAOBING ZOU, RUI LIU, NAIGONG ZENG, MIN HAN, JIANQIANG YUAN, XINXIN WANG, AND GUIXIN ZHANG

Department of Electrical Engineering, Tsinghua University, Beijing, China

(RECEIVED 1 July 2006; ACCEPTED 24 July 2006)

Abstract

A ~500 kV/400 kA/100 ns pulsed power generator (PPG-I) for x-pinch experiments was designed and constructed at Tsinghua University. It is composed of a Marx generator, a combined pulse forming line (PFL), a gas-filled V/N field distortion switch, a transfer line, and a copper-sulphate resistive load for testing. The PPG-I implements a novel design in lines that four pieces of waterline with impedance 5Ω in parallel constitute a combined PFL with 1.25Ω, and incorporate each other by a common self-break V/N switch on a matched 1.25Ω transfer line. At the peak charging voltage of the PFL, the V/N switch breaks down in multi-channel discharge mode, and electric energy is fed into the testing load through the 1.25Ω transfer line. This article presents the design and test of the PPG-I generator.

Keywords: Multi-channel discharge; Pulse forming line; Pulsed power; Rise time; X-pinch

1. INTRODUCTION

Between the output electrodes of a pulsed power generator, two or more wires crossing and touching at a single point constitute an "x" shape load. The cross position explodes first and then pinches axially to form the so-called x-pinch plasma, by the magnetic pressure as pulsed power generator delivers a suitable current to the "x" wires (Kalantar & Hammer, 1995; Shelkovenko *et al*., 1999). The x-pinch radiating intense X-ray pulse is an effective point source for X-ray backlighting in radiographing high-density z-pinch plasma.

Pulsed power devices play an important role in the production of high power particle beams and as intense sources of radiation for a variety of applications (Yatsui *et al*., 2005; Korobkin *et al*., 2005; Wang *et al*., 2005). In the last several years, inspired by the success of X-ray generation experiments on z-accelerator (Spielman *et al*., 1998; Deeney *et al*., 1998), wire array z-pinch plasma is being intensively studied. X-ray backlighting experiments are commonly used tools to diagnose dense plasma (Pikuz *et al*., 2004; Labate *et al*., 2004; Hartemann *et al*., 2004), and pulsed power machines have proved to be a reliable source of intense and hard X-ray radiation. To better understand the physics of z-pinches and to validate simulation models, experiments of X-ray backlighting to study exploding wires and wire array implosions were and are also being performed on BIN generator (~250 kA, 100 ns) at Lebedev Institute (Shelkovenko *et al*., 1999), XP pulsar (~480 kA, 100 ns) at Cornell University (Kalantar, 1993) and MAGPIE generator (~1.4 MA, 240 ns) at Imperial College (Mitchell *et al*., 1996).

Aimed at X-ray backlighting for exploding wires and wire array implosions, recently, a ~500 kV/400 kA/100 ns pulsed power generator (PPG-I) was designed and constructed at Tsinghua University. The PPG-I is composed of a Marx generator, a combined pulse forming line (PFL), a gas-filled V/N field distortion switch, a transfer line, and a copper-sulphate resistive load for testing. As a water-filled coaxial line with an impedance of ~5Ω has a highly insulating efficiency, the PPG-I performed a novel design in lines that four pieces of waterline with impedance 5Ω in parallel constitute a combined PFL with 1.25Ω, and incorporate each other by a common self-break V/N switch on a matched 1.25Ω transfer line. The novel lines design is unlike the MAGPIE generator lines design that four 5Ω PFLs each connects to its own triggered switch, and then incorporate each other by a single 1.25Ω transfer line, and also unlike the lines design of other traditional generators that a ~5Ω PFL connects to a switch on a taper line with a variable impedance. Being without triggered switches in parallel or taper line, the PPG-I will work more reliably or has a higher energy transmitting efficiency. The slower rise

Address correspondence and reprint requests to: Xiaobing Zou, Department of Electrical Engineering, Tsinghua University, Beijing 100084, China. E-mail: juxb@mail.tsinghua.edu.cn

time of output pulse in the PPG-I resulting from the lower driving impedance could be quickened by regulating the working state of V/N multi-channel switch.

This article presents the design and test of the PPG-I, and it is organized as follows: Section 2 generally describes the PPG-I and discusses the components design. Section 3 presents the calibration of voltage and current probes in the PPG-I. Waveforms derived with a copper-sulphate resistive load instead of x-pinch load are presented in Section 4. Section 5 concludes the design and test.

2. COMPONENTS DESIGN

2.1 General description of the PPG-I

As mentioned earlier, the PPG-I consists of a Marx generator, a combined pulse forming line (PFL), a gas-filled V/N field distortion switch, a transfer line, and a copper-sulphate resistive load for testing. Figure 1 represents a photograph of the PPG-I.

Typically, driving a single x-pinch load needs 100–250 kA peak current with 100–200 ns full width at half maximum (FWHM) (Kalantar & Hammer, 1995). The output parameters of PPG-I are designed to be ~500 kV, 400 kA, and 100 ns. It is appropriate for driving a source x-pinch in parallel with objective exploding wires for direct X-ray backlighting, or for driving two parallel source x-pinches to radiograph exploding wires or wire array implosions driven by another separate pulsar in two-frame mode. In addition to X-ray backlighting, The PPG-I is also intended to drive a puff-gas load (Zou *et al*., 2005, 2002), such as neon cylindrical load with a linear density of ~10 μg/cm. An applicable soft X-ray source will also be pursued on the PPG-I.

The normal output voltage V_M of Marx generator in the PPG-I is 1.2 MV. When Triggering pulse arrives, the Marx generator discharges in series, and charges the combined PFL synchronously. As the PFL reaches to its peak voltage V_F of about 1.09 MV (the voltage transfer efficiency between Marx and PFL is simulated to be about 91%), the auxiliary gap of V/N switch breaks down. Being distorted greatly with the electrical field between the main electrodes, the V/N switch swiftly breaks down in multi-channel mode, and then about $V_F/2$ pulses voltage is delivered to the matched transfer line. Decayed by transfer line, the pulse voltage ultimately fed to the load is about 500 kV. In the PPG-I, the combined PFL and transfer line both have 1.25 Ω characteristic impedance and 167cm length, which are fixed on by the output parameters of 400 kA peak current, 500 kV peak voltage and 100 ns duration time.

2.2. Marx generator

The PPG-I adopted Marx generator as its first-stage energy storage unit. For a total energy transfer, the series storage capacitance C_M of Marx generator should match C_F of PFL. C_F is given by

$$C_F = \frac{\tau}{2Z_F}, \tag{1}$$

where Z_F and τ are the characteristic impedance and pulse width of the combined PFL, respectively. Substituting 1.25 Ω for Z_F and 100 ns for τ to Eq. (1), it yields: C_F = 40nF; therefore, sixteen pieces of 0.66 μF/100 kV capacitor with the total series capacitance C_M of 41 nF were chosen for storage elements of the Marx generator. Marx circuit is presented in Figure 2.

Bipolar charge configuration was adopted, which could improve the charging efficiency and working reliability of the Marx generator. Two capacitors connected with a gas-filled spark gap constitute a charge and discharge module; there are such eight modules in the Marx generator. A

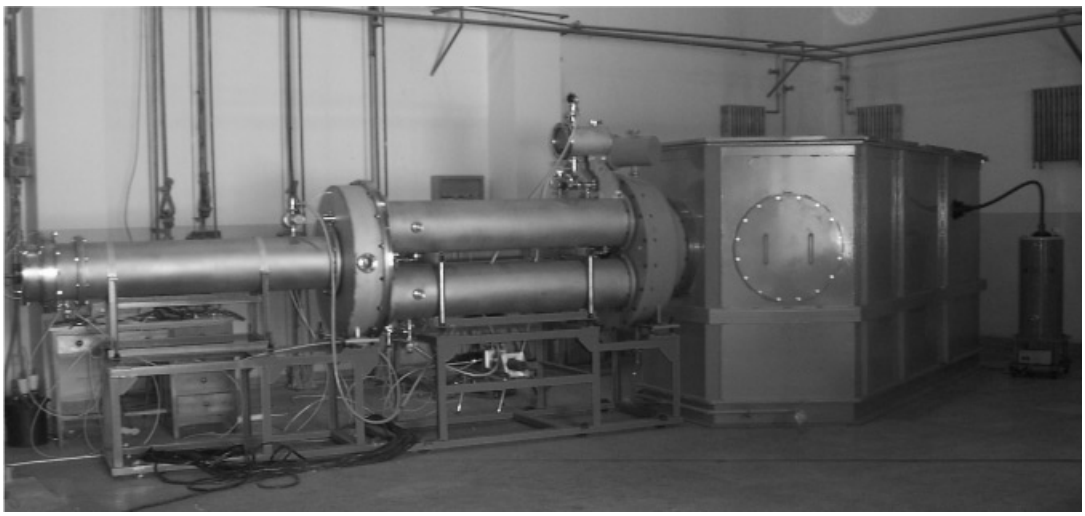

Fig. 1. View of the PPG-I.

https://doi.org/10.1017/S0263034606060666 Published online by Cambridge University Press

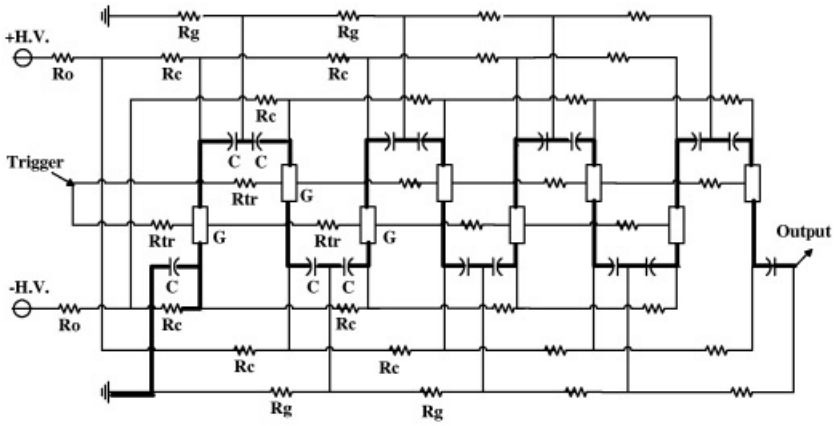

Fig. 2. Circuit of Marx generator.

triggering pulse of −160 kV with the rise time of 20 ns fires the first two spark gaps, and the rest spark gaps will be fired by resistance-coupling mode. All the capacitors are charged to +75 kV or −75 kV in parallel, thus the normal output voltage of the Marx generator is negatively 1.2 MV after being erected.

The Marx circuit was located on a PVC supporting shelf and immerged in a metallic tank filled with transformer oil. The results of three-dimensional electric field calculation (Liu *et al*., 2004) shows that the highest electric field E_{max} always appears at the sharp corner of the metallic shell of the last stage capacitor when the Marx generator discharges. In order to reduce partial field strength in the tank, metallic shields are mounted on all the capacitors to round the sharp corner.

Table 1 shows the parameters of the Marx generator. The erected inductance and series resistance are derived by the routine short-circuit experiment and charging experiment at 40kV charging voltage.

2.3. Pulse forming line-PFL and transfer line

Because of its high dielectric constant, de-ionized water (resistivity greater than $2 \times 10^4\ \Omega\cdot$m) was chosen as insulating material in coaxial transmission line. The stored energy scales with ε_r, while the wave speed scales with $\varepsilon_r^{-1/2}$, which means the transmission line filled with water can be shorter for a given pulse length. So for 100 ns given pulse duration in PPG-I, the length of all waterlines is dictated as 167 cm. The inner and outer radii of waterlines are determined by their insulating safety factors K_- and K_+,

$$K_- = \frac{E_-}{F_-}, \tag{2}$$

$$K_+ = \frac{E_+}{F_+}. \tag{3}$$

Above, E_- and E_+ are the surface field strengths of inner and outer cylinder, while F_- and F_+ are the negative and positive breakdown field strengths in water. E_- and E_+ can be derived from the following field strength formula for coaxial cylinder model

$$E = \frac{V}{r \ln \dfrac{R_2}{R_1}}, \tag{4}$$

where V is the applied voltage, R_1 and R_2 are the inner and outer radii of waterlines. F_- and F_+ in MV/cm are given by (Richard, 1991)

$$F_- = \frac{0.56\alpha}{A^{0.070} t_{\text{eff}}^{1/3}}, \tag{5}$$

$$F_+ = \frac{0.23}{A^{0.058} t_{\text{eff}}^{1/3}}. \tag{6}$$

Table 1. *The parameters of the Marx generator*

Capacitance (not erected)	$16 \times 0.66\ \mu$F
Total series capacitance	41 nF
Numbers of spark gap	8
Working charge voltage	75 kV
Working storage energy	29 kJ
Normal output voltage	1.2 MV
Series inductance	2.7 μH
Series resistance	~1.2Ω
Charging time for a 40 nF PFL	~740 ns

https://doi.org/10.1017/S0263034606060666 Published online by Cambridge University Press

Above, A is the stressed area in cm^2, and t_{eff} is the effect stressed time in μs, the time that the pulse is above 63% of peak voltage. α is the field enhancement factor given by

$$\alpha = 1 + 0.12[(E_{\max}/E_{\text{mean}}) - 1]^{1/2}, \quad (7)$$

$E_{\max}$ and E_{mean} could be derived from Eq. (4).

Based on Eqs. (2)–(7), Table 2 shows the calculated K_- and K_+ for different impedance waterlines with different inner and outer radii while the inner is negatively charged to 1.09 MV within 740 ns.

Generally, the safety factor is designed to be below 0.7. As shown in Table 2, the K_- and K_+ for a 5 Ω waterline are both nearly to be 0.5, while for a 1.25 Ω waterline K_+ might be below 0.7 only the outer diameter closes to 100 cm.

Insulating diaphragms used to support the inner cylinder at the both terminals of waterline are very expensive when the diameter exceeds 100 cm. In order to heighten the insulating efficiency and reduce the cost of PFL, a novel lines configuration in the PPG-I is performed as follows: Four 5Ω waterlines in parallel each with 14.6 cm inner diameter and 30.9 cm outer diameter constitute the combined 1.25Ω PFL, and incorporate each other by a common self-break V/N switch on a matched 1.25Ω transfer line. The novel design of lines, shown in Figure 3, differs from the MAGPIE generator lines design that four 5Ω PFLs each connects to its own triggered switch, and then incorporate each other by a single 1.25Ω transfer line, and also differs from the lines design of other traditional generators that a ~5 Ω PFL directly connects to a switch on a taper line with a variable impedance. Being without triggered switches in parallel or taper line, the PPG-I will work more reliably or has a higher energy transmitting efficiency. The slower rise time of output pulse in the PPG-I resulting from the lower driving impedance should be quickened by regulating the working state of V/N multi-channel switch

As shown in Figure 3, at both terminals of all the 5Ω PFLs, each inner cylinder traverses an insulating diaphragm and connects to an incorporated plate. To reduce the electric field adjacent to the insulating diaphragm, the diameter of the inner PFLs at the diaphragm is reduced to 10.6 cm, while the outer PFLs increased to 33.9 cm. The special shape keeps the mean electric field across the insulating diaphragms below 110 kV/cm allowed in general design guide for fields across the insulating supports.

Table 2. K_- and K_+ for different impedance waterlines with different inner and outer radii

Impedance (Ω)	R_1 (cm)	R_2 (cm)	K_+	K_-
1.25	41.5	50	0.66	0.38
5	7.3	15.45	0.49	0.49

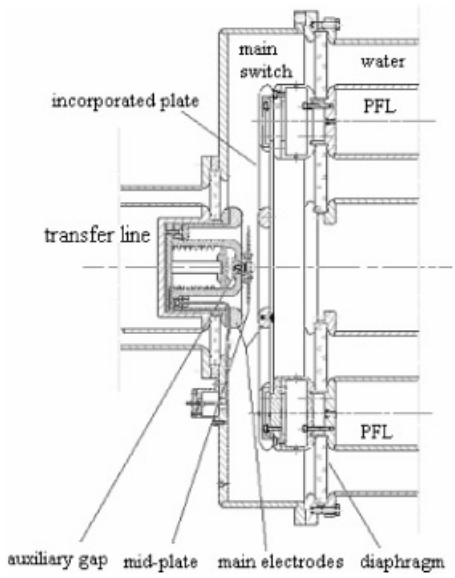

Fig. 3. Connections of the combined PFL, the V/N switch, and the transfer line.

The 1.25Ω transfer line, with 25.6 cm inner and 30.9 cm outer diameters, delivers electric power from the combined PFL to the load and is also employed to reduce the prepulse voltage reaching the load as the PFL is charged. Stressed about $V_F/2$ voltage with the duration time of 100 ns, the positive and negative insulating safety factors of the transfer line are respectively 0.66 and 0.38, and the line length is chosen to be 167 cm so that the pulse reflection from load can be delayed until after the main pulse begins to turn off.

2.4. Main switch

A pressurized gas-filled self-break V/N switch shown in Figure 3 is employed in the PPG-I. When the power electrode is charged to V_F, the auxiliary gap self-breaks down first, and then greatly distorted and enhanced fields at the edges of the mid-plate swiftly initiate the discharge across the main electrodes.

Ignoring the resistive phase time, the rise time $t_{10\%-90\%}$ of the V/N switch is determined by

$$t_{10\%-90\%} \approx 2.2\tau_l = \frac{2.2L}{Z}, \quad (8)$$

where τ_l are the inductive phase time constant; L and Z are the switch inductance and driving impedance, respectively. In the PPG-I, the V/N switch drives low impedance including the 1.25Ω PFL and 1.25Ω transfer line. In order to achieve a fast rise time, the total inductance L of V/N switch roughly determined by the number of breakdown channels n must be small enough. Table 3 shows the calculation results of $t_{10\%-90\%}$ and L vs. n. From Table 3 we know that if n is not less than 4, $t_{10\%-90\%}$ would be faster than 40 ns.

https://doi.org/10.1017/S0263034606060666 Published online by Cambridge University Press

Table 3. *The calculation results of $t_{10\%-90\%}$ and L vs. n*

n (channels)	1	4	6	8
L (nH)	108.5	51.7	45.4	42.3
$t_{10\%-90\%}$ (ns)	72.2	40.0	35.9	33.4

3. CALIBRATIONS OF VOLTAGE AND CURRENT PROBES

To facilitate monitoring of machine operation and fault diagnosis, voltage and current probes were installed in the PPG-I. Capacitive voltage dividers were located at both terminals of all the 5Ω PFLs and the output terminal of the transfer line for measuring the charging voltage and load voltage, respectively. At the output terminal of the transfer line nearly adjacent to the load, a current wall monitor made of stainless steel was also placed to monitor the load current.

All the voltage and current probes in waterlines should be calibrated in situ. A well-connected calibration design was shown in Figure 4, which can be used for calibrating probes in transfer line as well as in PFLs.

To calibrate the probes in transfer line, a special taper waterline with constant impedance of 1.25Ω (or 5Ω for calibrating probes in PFLs) was designed to transit the source pulse. As shown in Figure 4, the output pulse *Vp* (∼ a few kilovolts) of a source pulsar is divided to two *V*p/2 equal pulses by a power divider. One *Vp*/2 pulse is directly fed to oscilloscope as reference signal, and another *Vp*/2 pulse through an impedance convertor (50Ω–1.25Ω) and the 1.25Ω taper waterline is fed to the object transfer line. Comparing the reference signal with the electric signals of voltage divider and current viewing resistor, the voltage division ratio and accurate resistive value can be derived.

4. SYSTEM PERFORMANCE

An adjustable copper-sulphate resistive load is used to scale the output of the PPG-I. By varying the gas pressures respectively in main gap and auxiliary gap, the V/N switch would breaks down near the peak voltage in multi-channel or single-channel discharge mode. Extensive tests have been made to study the relationship between the rise-time of the output voltage pulse and the number of spark channels inside the V/N switch. Figure 5 shows the typical multi-channel and single-channel photographs observed by a digital camera. The output voltage and current waveforms corresponding to Figure 5 are shown in Figure 6. In the experiments, the operating voltage of Marx generator keeps being 75 kV, and the testing load is adjusted to ∼1.25Ω.

From the charging voltage trace of the PFL in Figure 6, it can be seen that The V/N switch breaks down at about 700 ns related to the start of the charging voltage, and the load voltage and current of the PPG-I are, respectively, 46 0kV and 380 kA with about 110 ns FWHM.

Results based on a series of experiments show us that the rise-time of the output voltage pulse is closely related to the number of the spark channels, ∼70 ns for one spark channel and ∼30 ns for 6–7 spark channels.

5. CONCLUSION

A ∼500 kV/400 kA/100 ns pulsed power generator (PPG-I) for x-pinch experiments was designed and constructed at Tsinghua University. It is based on an oil-insulated 16-stages Marx generator which stores 29 kJ at 75 kV operating voltages. After being erected, the Marx produces a 1.2 MV pulse to charge a combined 1.25Ω PFL composed of four 5Ω coaxial waterlines in parallel in about 700 ns. A pressurized self-break V/N switch working in multi-channel discharge mode connects the combined PFL to a matched

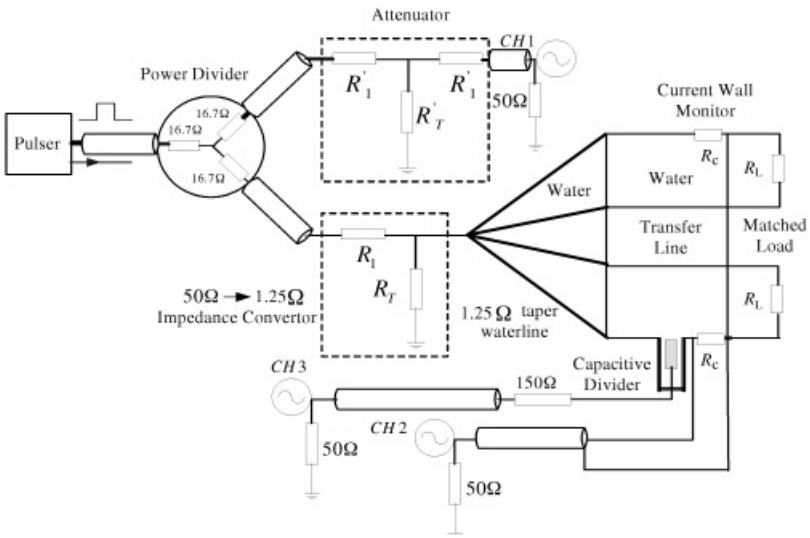

Fig. 4. Calibration circuit for the voltage and current probes in transfer line.

https://doi.org/10.1017/S0263034606060666 Published online by Cambridge University Press

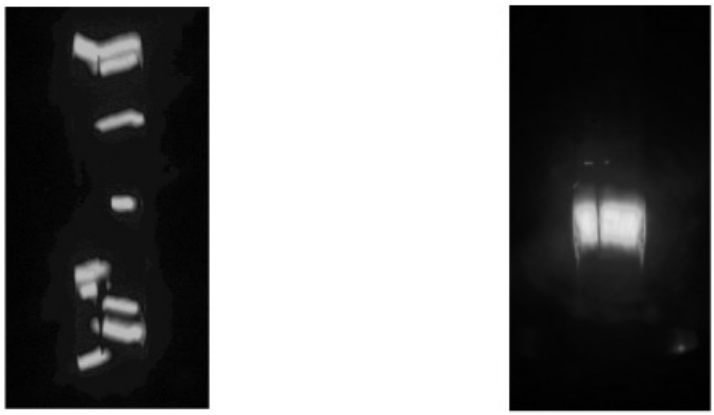

(a) V/N switch works in multi-channel mode with pressures of 0.46Mpa in main gap and 0.27Mpa in auxiliary gap

(b) V/N switch works in single-channel mode with pressures of 0.46Mpa in main gap and 0.34Mpa in auxiliary gap

Fig. 5. Spark channels inside the V/N switch. In Figs. 5a and 5b, the cathode (high voltage electrode) is at the right side and the anode at the left. Mid-plate (self-break plate) slightly near the anode crosses all the spark channels

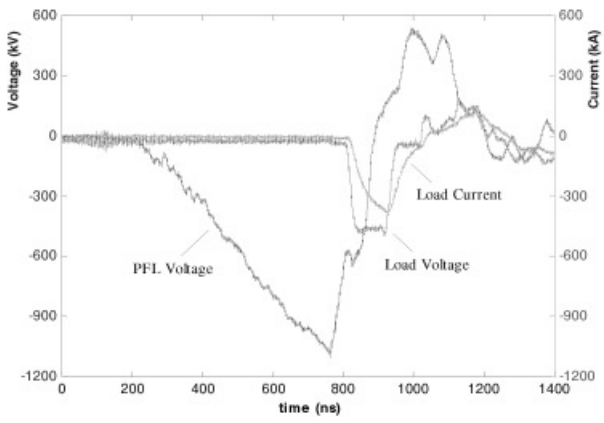

Fig. 6. The output voltage and current waveforms on a ~1.25Ω load.

1.25Ω transfer line. Capacitive voltage dividers and current wall monitor were located on different points of the lines to measure the voltage and current pulses. Extensive tests have been made to scale the output of the PPG-I when operating with an adjustable copper-sulphate resistive load. From the calibrated monitors the load voltage and current of the PPG-I are respectively 460 kV and 380 kA with about 110 ns FWHM.

ACKNOWLEDGMENTS

Project supported by Tsinghua Basic Research Foundation (Grant No. 200109001), and the IAEA under Research Contract 12409/RBF, and by China Postdoctoral Science Foundation (Grant No. 2004035002).

REFERENCES

Deeney, C., Douglas, M.R., Spielman, R.B., Spielman, RB., Rash, T.J., Peterson, D.L., L'Eplattenier, P., Chandler, G.A., Seamen, J.F. & Sturve, K.W. (1998). Enhancement of X-ray power from a Z pinch using nested-wire arrays. *Phys. Rev. Lett.* **81**, 4883–4886.

Hartemann, F.V., Tremaine, A.M., Anderson, S.G., Barty, C.P.J., Betts, S.M., Booth, R., Brown, W.J., Crane, J.K., Cross, R.R., Gibson, D.J., Fittinghoff, D.N., Kuba, J., Le Sage, G.P., Slaughter, D.R., Wootton, A.J., Hartouni, E.P., Springer, P.T., Rosenzweig, J.B. & Kerman, A.K. (2004). Characterization of a bright, tunable, ultrafast Compton scattering X-ray source. *Laser Part. Beams* **22**, 221–244.

Kalantar, D.H. (1993). An experimental study of the dynamics of X-pinch and Z-pinch plasmas. Ph.D. Thesis. Ithaca, NY: Cornell University Press.

https://doi.org/10.1017/S0263034606060666 Published online by Cambridge University Press

Kalantar, D.H. & Hammer, D.A. (1995). The x-pinch as a point-source of X-rays for backlighting. *Rev. Sci. Instrum.* **66**, 779–781.

Korobkin, Y.V., Romanov, I.V., Rupasov, A.A., Shikanov, A.S., Gupta, P.D., Khan, R.A., Kumbhare, S.R., Moorti, A. & Naik, P.A. (2005). Hard X-ray emission in laser-induced vacuum discharge. *Laser Part. Beams* **23**, 333–336.

Labate, L., Galimberti, M., Giulietti, A., Giulietti, D., Gizzi, L.A., Koster, P., Laville, S. & Tomassini, P. (2004). Ray-tracing simulations of a bent crystal X-ray optics for imaging using laser-plasma X-ray sources. *Laser Part. Beams* **22**, 253–259.

Liu, R., Zeng, N.G. & Wang, X.X. (2004). An insulation design for a 1.2 MV enclosed Marx generator. *Proc. 12th Asian Conference on Electrical Discharge*, pp. 678–680. Beijing, China: Tsinghua University Press.

Mitchell, I.H., Bayley, J.M., Chittenden, J.P., Worley, J.F., Dangor, A.E., Haines, M.G. & Choi, P. (1996). A high impedance mega-ampere generator for fiber z-pinch experiments. *Rev. Sci. Instrum.* **67**, 1533–1541.

Pikuz, T., Faenov, A., Skobelev, I., Magunov, A., Labate, L., Gizzi, LA., Galimberti, M., Zigler, A., Baldacchini, G., Flora, F., Bollanti, S., Di Lazzaro, P., Murra, D., Tomassetti, G., Ritucci, A., Reale, A., Reale, L., Francucci, M., Martelluci, S. & Petrocelli, G. (2004). Easy spectrally tunable highly efficient X-ray backlighting schemes based on spherically bent crystals. *Laser Part. Beams* **22**, 289–300.

Richard, J.A. (1991). *Pulse Power Formulary*. Albuquerque, NM: North Star Research Corporation.

Shelkovenko, T.A., Pikuz, S.A., Hammer, D.A., Dimant, Y.S. & Mingaleev, A.R. (1999). Evolution of the structure of the dense plasma near the cross point in exploding wire X pinches. *Phys. Plasmas* **6**, 2840–2846.

Spielman, R.B., Deeney, C., Chandler, G.A., Douglas, M.R., Fehl, D.L., Matzen, M.K., McDaniel, D.H., Nash, T.J., Porter, J.L., Sanford, T.W.L., Seamen, J.F., Stygar, W.A., Struve, K.W., Breeze, S.P., McGurn, J.S., Torres, J.A., Zagar, D.M., Gilliland, T.L., Jobe, D.O., McKenney, J.L., Mock, R.C., Vargas, M., Wagoner, T. & Peterson, D.L. (1998). Tungsten wire-array Z-pinch experiments at 200 TW and 2 MJ. *Phys. Plasmas* **5**, 2105–2111.

Wang, X.X., Hu, Y. & Song, X.H. (2005). Gas discharge in a gas peaking switch. *Laser Part. Beams* **23**, 553–558.

Yatsui, K., Shimiya, K., Masugata, K., Shigeta, M. & Shibata, K. (2005). Characteristics of pulsed power generator by versatile inductive voltage adder. *Laser Part. Beams* **23**, 573–581.

Zou, X.B., Wang, X.X., Luo, C.M. & Han, M. (2005). Experimental study of gas-puff z-pinch plasma. *Plasma Sour. Sci. & Technol.* **14**, 268–272.

Zou, X.B., Wang, X.X., Luo, C.M. & Han, M. (2002). Measuring the gas flow from a supersonic nozzle used in a 1.5-MA gas puff Z pinch. *IEEE Trans. Plasma Sci.* **30**, 482–487.